Available online at www.sciencedirect.com
ScienceDirect
Materials Letters 61 (2007) 4752–4755
materials letters
www.elsevier.com/locate/matlet

N-doped ZnO nano-arrays: A facile synthesis route, characterization and photoluminescence

Wei-Tai Wu [a,b], Lei Shi [a], Qingren Zhu [a,*], Yusong Wang [a], Guoyong Xu [a], Wenmin Pang [a]

[a] *Hefei National Laboratory for Physical Sciences at the Microscale, Structure Research Laboratory, University of Science and Technology of China, Chinese Academy of Sciences, Hefei 230026, China*
[b] *Department of Electrical Engineering, The Hong Kong Polytechnic University, Hong Kong SAR, China*

Received 25 January 2007; accepted 4 March 2007
Available online 14 March 2007

Abstract

Field emission scanning electron microscopy (SEM) investigation reveals that array-orderly novel nanostructures, which are nanorods with many nanoparticles on the surfaces, have been synthesized at low temperature (162 °C) via a one-step *in-situ* process in solution. High resolution transmission electron microscope (HRTEM) and energy-dispersive X-ray spectroscopy (EDS), coupled with X-ray powder diffraction (XRD) patterns and X-ray photoelectron spectra (XPS), reveal that the as-obtained products possess crystalline structure of N-doped ZnO. The room temperature photoluminescence (PL) spectrum has also been examined to explore the optical property. The present synthesis method possesses several advantages, which would be significant to be studied deeper in the future. It is also envisioned that this method could provide a new approach to synthesize ZnO:N and other ZnO-based adulterants at low temperature.

Keywords: Nanomaterials; ZnO; Microstructure; Photoluminescence

1. Introduction

Considerable attention has been focused recently on ZnO due to its applications in short-wavelength light emitter and detector, etc. [1]. However, the realization of p-type ZnO, which is critical to practical applications of ZnO-based devices, has proven difficult and thought to be the bottleneck in the development of ZnO-based devices due to the asymmetric doping limitations in ZnO [2,3]. Recently, N has proven to be a suitable acceptor for making p-type ZnO [4], and N-doped ZnO (ZnO:N) has been fabricated by various deposition methods [5–8]. Nevertheless, it seems that all attempts in obtaining ZnO:N have not been quite successful so far, because the affinity of O is higher than that of N [9]. Note that for the ZnO:N synthesis reported previously, usually a growth temperature above 300 °C is needed; unfortunately, the incorporation of N into ZnO is difficult at such a high temperature, and the N concentration decreases rapidly as the temperature increases [10]. These techniques also come with a high cost (problems with scale-up and high-energy consumption, and expensive instruments). So, the preparation of ZnO:N with high purity and at low cost calls for a simpler and more tractable route.

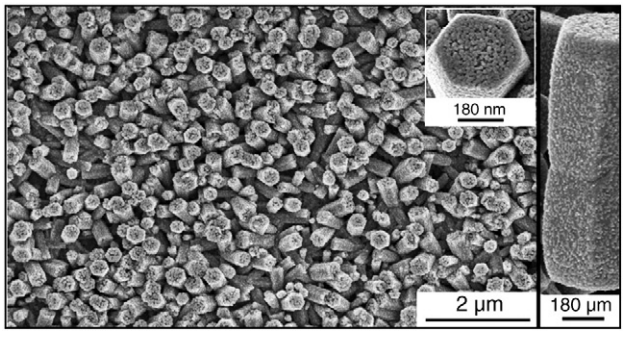

Fig. 1. Typical SEM images of ZnO:N oriented nano-array grown onto Cu substrate.

* Corresponding author. Tel.: +86 551 3602813; fax: +86 551 3602803.
E-mail address: zhuqr@ustc.edu.cn (Q. Zhu).

0167-577X/$ - see front matter © 2007 Elsevier B.V. All rights reserved.
doi:10.1016/j.matlet.2007.03.020

The control of the shape and the orientation of nano-/microstructures, in particular the ability to order them into three-dimensional (3D) arrays onto various types of substrates, represent essential tasks to create functional materials. Owing to their promising applications, 3D ZnO nanorod arrays have been prepared by various methods [11,12]. However, report about array-orderly ZnO:N nano-/microstructures, to the best of our knowledge, is rare.

In this letter, we report a facile route to synthesize array-orderly ZnO:N nanostructures on copper substrate at 162 °C, via a one-step *in-situ* process in solution. This temperature for the synthesis is much lower than that previously reported in ZnO:N synthesis [5–8]. In addition, this is the first, to the best of our knowledge, report about the present novel nanostructures which are nanorods with many nanoparticles on the surfaces. The reaction can be described as follows:

$$Zn^{2+} + NH_3 \rightarrow Zn(NH_3)_4^{2+} \xrightarrow[\text{ethyleneglycol}]{162\ ^\circ C} ZnO : N$$

2. Experiments

3.040 g of $ZnCl_2$ was dissolved in 100 ml of ethylene glycol, and 13 ml of ammonia was added (25%) to adjust the pH value to 10.0. The solution was poured into a 250 ml round-bottomed flask equipped with condenser pipe. Copper foils (≥99.8%) with a thickness of 0.1 mm, cleaned with acetone and deionized water in an ultrasonic cleaner, were placed inside. The flask was heated at 162 °C for 90 min without stirring, then cooled down to room temperature naturally. The product was washed with acetone, deionized water and ethanol repeatedly, and dried in air. The microstructure was characterized by scanning electron microscopy (FEI Sirion 200 FEG SEM) and transmission electron microscopy (JEOL-2010 HRTEM). XRD patterns were recorded on a MAC Science Co. Ltd. MXP 18 AHF X-ray diffractometer with monochromatized Cu Kα radiation ($\lambda = 1.54056$ Å). XPS spectra were obtained with a VG Smart IQ^+ Thermo Electron Co. ESCALAB 250 XPS spectrometer. PL spectra were obtained on a Jobin Yvon Co. Fluorolog-3-Tau Steady-state/Lifetime Spectrofluorometer.

3. Results and discussion

As shown in Fig. 1, aligned hexagonal rods of about 180 nm in width and 1.2 μm in length were grown and mostly oriented in a perpendicular fashion onto the substrate and arranged in very large areas. Interestingly, closer inspection revealed that the surface of those

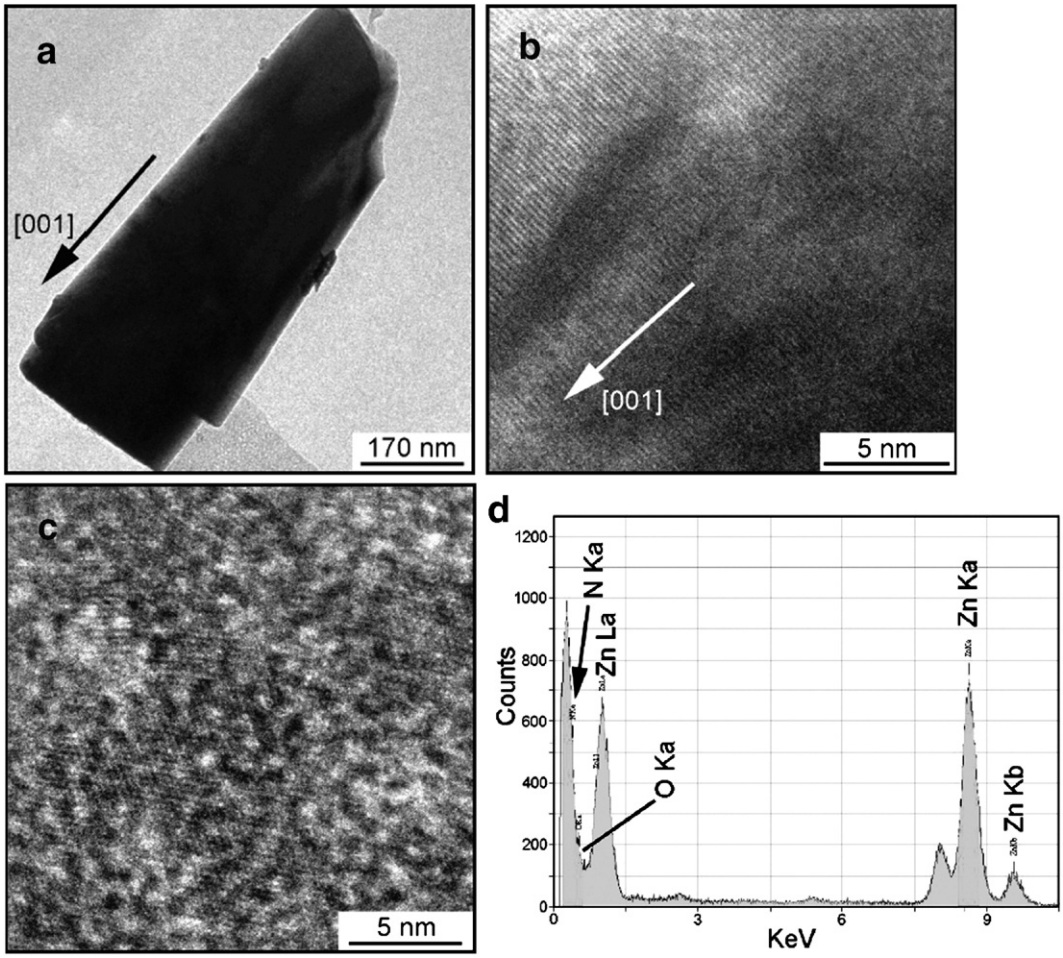

Fig. 2. (a) Typical TEM image of ZnO:N nanostructures. HRTEM images of (b) the nanorod region, and (c) the surface nanoparticle region. (d) Corresponding EDS spectrum.

nanorods is coated with monolayer smaller nanoparticles with an average diameter of 20 nm. Lattice-resolved HRTEM image of the nanorods (Fig. 2) shows the parallel strips. Further examination finds that most regions (the region >20 nm away from the surface, >80%) have a lattice spacing of 2.58 Å; however, the lattice spacing increases gradually to ~2.59 Å toward outward regions (from ~8 nm deep to the surface). The nanoparticles coated on the surface of the nanorods have nearly the same lattice spacing of 2.58 Å (Fig. 2c). Whatever, the observed lattice spacing is always a little smaller than 2.602 Å corresponding to the (002) plane for the undoped ZnO (JCDP card no. 05-0664); this result coincides with that shown by XRD patterns (see Electronic Annex), as revealed by the shift of the (002) diffraction peak to 2.589 Å, and the extracted *c*-axis lattice constant decreasing to 5.181 Å accordingly. Thus, the observed lattice spacing possibly corresponds to the (002) plane for the ZnO:N phase, indicating that the dopants have integrated into the lattice sites, and an individual nanorod grows preferentially along the [001] direction [7,13]. For the decreasing *c*-axis lattice constant in ZnO:N, one reason is that Zn–N has a shorter bond-length than Zn–O, however, this difference is relatively small; the main reason is compressive stress, which is contributed by excessive N, randomly distributed in the lattice, and an additional collapse of Zn tetrahedrons around oxygen sites [3]. Furthermore, the incorporation of N into the ZnO crystals was also proved by the EDS analysis of the nanostructures, which reveals the presence of N (Fig. 2d).

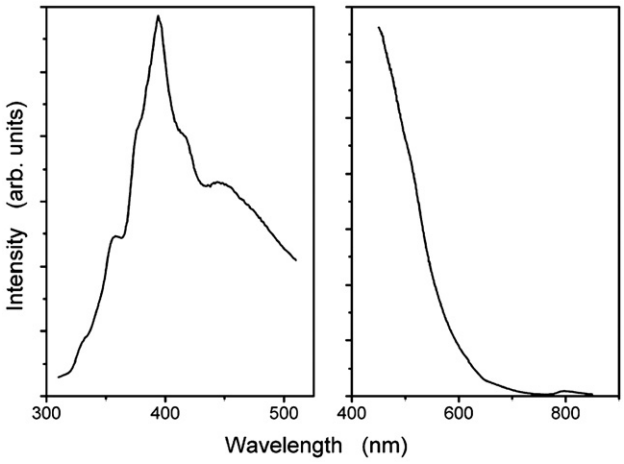

Fig. 4. PL spectra of as-prepared ZnO:N, λ_{ex}=273 nm.

The samples were also characterized by XPS. Three peaks at the binding energies of 405.0, 400.4 and 397.2 eV are detected in the N_{1s} region (Fig. 3a). The 400.4 and 405.0 eV peaks could be assigned to terminally bonded well screened and poorly screened γ-N_2 states, respectively, one of which is a N_2 molecule occupying a position on the oxygen sublattice and should be a shallow double donor, and they are at

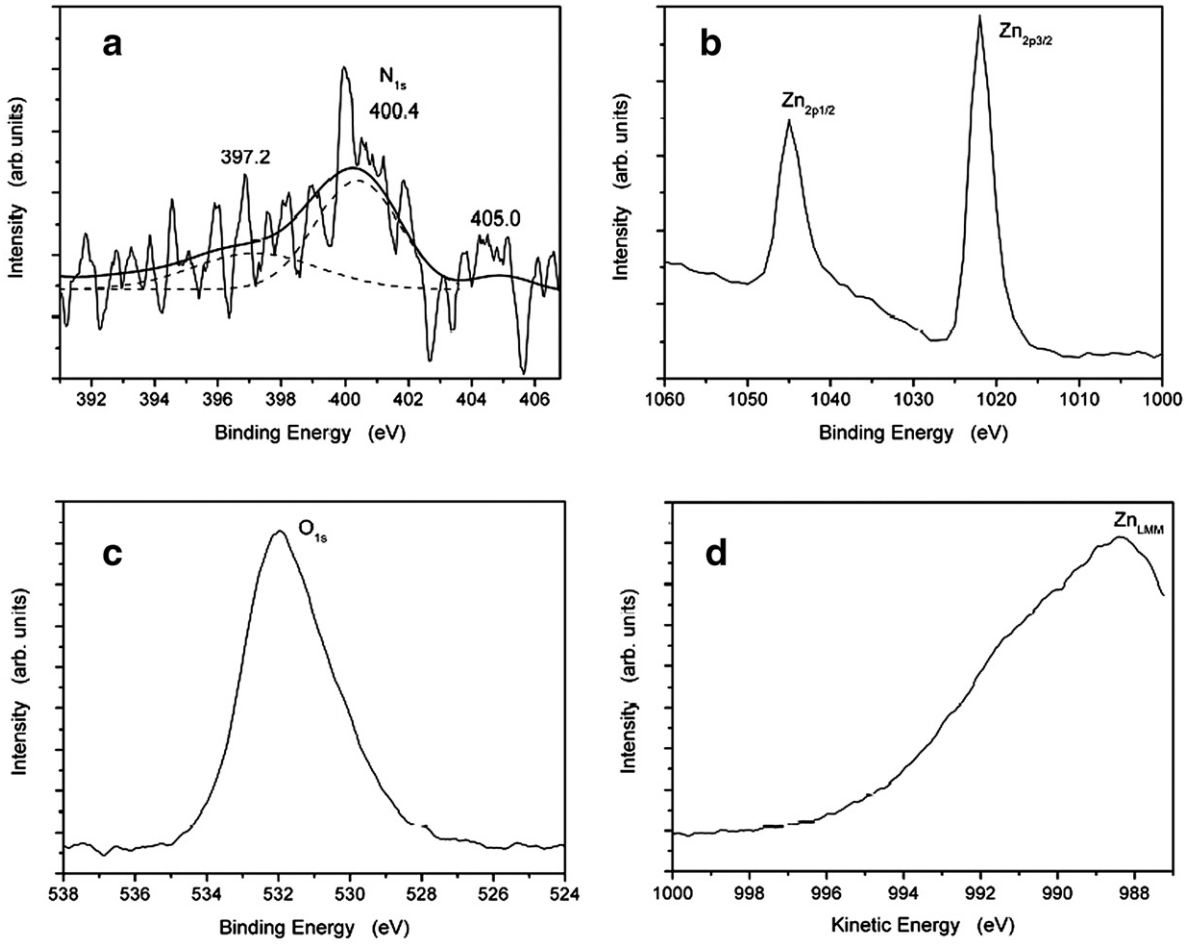

Fig. 3. XPS spectra of (a) N_{1s}, (b) Zn_{2p} and (c) O_{1s} regions of as-prepared ZnO:N. (d) The Auger line of the Zn_{LMM} region.

a level somewhat below the surface rather than right at the surface [14]. The peak at 397.2 eV indicates the successful incorporation of N into the lattice, as this peak is often ascribed to N^{3-} in Zn–N bonding, in which N has received substantial charge from the surrounding metal atoms, being the desired acceptor [13,14]. The $Zn_{2p3/2}$ and $Zn_{2p1/2}$ binding energies are 1021.6 and 1045.0 eV, respectively (Fig. 3b). The $Zn_{2p3/2}$ kinetic energy is 988.4 eV (Fig. 3d), and the modified Auger parameter α' is 2010.0 eV. The chemical state of Zn could indirectly reflect the bonding state of N and the relative quantity of Zn–N, and the results are consistent with those reported previously [13–15]. Moreover, no peak due to Cu ($Cu_{2p3/2}$ ~ 933 eV [16]) was observed.

Room temperature PL spectra (Fig. 4) were also performed to explore the optical property, showing two weak emission bands at 359 nm (3.45 eV) and ~445 nm (~2.79 eV), a stronger and narrower ultraviolet emission at 394 nm (3.15 eV), and two humps at ~376 nm (~3.30 eV) and 416 nm (2.98 eV), etc. The emission at 359 nm is the UV near-band-edge emission that is attributed to the photogenerated electron from the conduction band to the valence band, which is influenced strongly by the surface defect considering the large surface-to-volume ratio of nanoparticles [17]. The broad emission centered at ~445 nm is the deep level emission, which is due to a transition of a photogenerated electron from the conduction band to a deeply trapped hole, and the probable candidate for the trapping of holes is the O^{2-}/O^{-} ion at the surface [18]. The strong emission at 394 nm possibly originated from the electron transition from shallow donor levels of oxygen vacancies and doping N atoms to the top of valence band levels [2]. The hump at 376 nm is generally accepted as the "fingerprint" for N-doping in ZnO; its assignment is contentious, but most authors ascribe the peak to an acceptor-bound exciton [2,8,17,18]. In addition, other weak peaks at 331, 416 nm, etc. may be associated with certain free exciton recombination and structure defects.

4. Conclusion

Array-orderly novel nanostructures have been synthesized through a facile one-step solution route at low temperature (162 °C). The products possess the crystalline structure of ZnO:N. PL spectrum has also been examined to explore the optical property. This method possesses several advantages, for example, at low temperature, contamination is easy to remove. It is also a simple and low cost process, with new morphology and array patterns, and capable of large area fabrication with good uniformity. These advantages, together with the luminescence, would be significant to be studied deeper in the future. It is also envisioned that this route could provide a new approach to synthesize ZnO:N and other ZnO-based adulterants at low temperature.

Acknowledgement

This work is supported by the Innovation Foundation of USTC for the Postgraduate.

Appendix A. Supplementary data

Supplementary data associated with this article can be found, in the online version, at doi:10.1016/j.matlet.2007.03.020.

References

[1] Z.L. Wang, Annu. Rev. Phys. Chem. 55 (2004) 159.
[2] H. Wei, Y. Wu, L. Wu, C. Hu, Mater. Lett. 59 (2005) 271.
[3] C.H. Park, S.B. Zhang, S.H. Wei, Phys. Rev., B 66 (2002) 073202.
[4] A. Kobayashi, O.F. Sankey, J.D. Dow, Phys. Rev., B 28 (1983) 946.
[5] G. Du, Y. Ma, Y. Zhang, T. Yang, Appl. Phys. Lett. 87 (2005) 213103.
[6] L. Chen, J. Lu, Z. Ye, Y. Lin, B. Zhao, Y. Ye, J. Li, L. Zhu, Appl. Phys. Lett. 87 (2005) 252106.
[7] Y. Nakano, T. Morikawa, T. Ohwaki, Y. Taga, Appl. Phys. Lett. 88 (2006) 172103.
[8] Y.J. Zeng, Z.Z. Ye, W.Z. Xu, B. Liu, Y. Che, L.P. Zhu, B.H. Zhao, Mater. Lett. 61 (2007) 41.
[9] P. Fons, H. Tampo, S. Niki, A.V. Kolobov, M. Ohkubo, J. Tominaga, S. Friedrich, R. Carboni, F. Boscherini, Nucl. Instrum. Methods Phys. Res., B Beam Interact. Mater. Atoms 246 (2006) 75.
[10] M. Sumiya, S. Fuke, A. Tsukazaki, K. Tamura, A. Ohtomo, M. Kawasaki, H. Koinuma, J. Appl. Phys. 93 (2003) 2562.
[11] X. Feng, L. Feng, M. Jin, J. Zhai, L. Jiang, D. Zhu, J. Am. Chem. Soc. 126 (2004) 62.
[12] L.E. Greene, M. Law, D.H. Tan, M. Montano, J. Goldberger, G. Somorjai, P. Yang, Nano Lett. 5 (2005) 1231.
[13] T.M. Barnes, J. Leaf, S. Hand, C. Fry, C.A. Wolden, J. Appl. Phys. 96 (2004) 7036.
[14] C.L. Perkins, S.H. Lee, X. Li, S.E. Asher, T.J. Coutts, J. Appl. Phys. 97 (2005) 034907.
[15] G. Cong, W. Peng, H. Wei, X. Han, J. Wu, X. Liu, Q. Zhu, Z. Wang, J. Lu, Z. Ye, L. Zhu, H. Qian, R. Su, C. Hong, J. Zhong, K. Ibrahim, T. Hu, Appl. Phys. Lett. 88 (2006) 062110.
[16] C.D. Wagner, W.M. Riggs, L.E. Davis, J.F. Moulder, G.E. Muilenberg, Handbook of X-ray Photoelectron Spectroscopy, Perkin-Elmer Corporation, Eden Prairie, Minnesota, 1979.
[17] R.F. Service, Science 276 (1997) 895.
[18] A. Van Dijken, E.A. Meulenkamp, D. Vanmaekelbergh, J. Phys. Chem., B 104 (2000) 1715.